MODELS FOR PIGMENT PATTERN FORMATION IN THE SKIN OF FISHES

K.J. PAINTER
DEPARTMENT OF MATHEMATICS, UNIVERSITY OF UTAH, SALT LAKE CITY, UT 84112, USA.

Abstract. The colours and patterns of the skin provides a fascinating system used for the study of pattern formation in experimental and theoretical research alike. In this article, a brief review of recent work on the pigmentation of the skin is presented. A mathematical model is shown to be able to capture many features associated with the evolving colour patterns on juveniles belonging to the genus of marine angelfish, *Pomacanthus*. Different forms of growth lead to very different patterning phenomena. The development of computational tools which can accurately reflect the geometry and growth of the real system will allow the studying of the relationship between growth and patterning in species such as *Pomacanthus* or zebrafish.

1. Introduction.

Across the animal kingdom, a large number of species rely on the colours and markings of their skin for purposes such as concealment and warning. The sophistication and control has reached astonishing levels in some animals. For example, species of bottom dwelling flatfish have been shown to adapt rapidly to background shades [53] and can assume a checkerboard type pattern when placed on the appropriate surface [45].

The ability to change skin colour and pattern is essential for survival in many species. In species such as the flatfish or the chameleon, the change occurs rapidly (on the order of seconds): such changes are termed *physiological* colour changes and are controlled by hormonal or nerve signals. The more slowly evolving changes are termed *morphological* colour changes, and these occur in response to continuous exposure to stimuli, as can be seen by prolonged exposure of skin to sunlight. A particularly striking example occurs in members of the marine angelfish genus *Pomacanthus* [14, 15]. Several species of *Pomacanthus* display a similar juvenile pattern consisting of several curved vertical white bars on a dark blue background. As the fish grows in size, new white bars are added between the older stripes, first emerging faint and narrow but widening as the fish continues to grow. This process repeats once or twice before the pattern evolves to the adult form, which can vary drastically between species. The aggressive adults attack fish with similar color patterns, and therefore juveniles adopt a distinctly different pattern to allow them to safely swim in an adults territory, [16].

The relationships between age, growth and patterning have attracted interest from experimentalists and theoreticians alike. A simple one-dimensional model

based on a Turing mechanism [61] was proposed to account for basic aspects of pattern evolution in the above angelfish [29], and further extensions have been incorporated to account for patterning details [62, 50]. An experimental study of a link between growth and patterning in members of the genus *Danio* (which includes the much studied zebrafish) has also been undertaken [35].

Pigment cells contain natural cell markers, namely, the pigment itself, and thus studies of pigmentation have provided experimentalists with a valuable system for understanding pattern formation in the developing embryo. In addition, studying these mechanisms may have important consequences for the clinical sciences. A number of diseases are attributed to defective pigmentation, including the condition vitiligo which affects approximately 1% of the population. This disease is a result of destruction of melanocytes and causes patches of white skin. Understanding the mechanisms by which pigment cells migrate and proliferate to pattern the skin may lead to a more successful course of treatment.

In this paper we present a brief review of the recent experimental and modelling research on the development of patterns and colours. We proceed to present a number of mathematical models for pigmentation in species of fish.

2. Formation of pigment patterns.

A great body of research exists on the physiology of pigment cells and the formation of patterns within the skin. We refer to the following for greater detail: [10, 55, 12, 18, 17].

2.1. Pigments and chromatophores.

Colour and pattern is the result of pigment cells (also called chromatophores) in the dermal and epidermal skin layers. These cells are large, branched and highly motile and contain membrane organelles called chromosomes holding the pigment granules. The organelles are rapidly aggregated or dispersed in response to nerve or hormonal signals. A number of chromatophore types exist, corresponding to the different pigments and colour. These include,

- *Melanophores* are a common chromatophore type residing in dermal and epidermal skin layers. In mammals and birds, they reside in the dermis where they are responsible for oranges and blacks by the transfer of pigment from melanophore dendrites into hairs, feathers and epithelial cells. In fish, melanophores give rise to black pigmentation, and are found in the dermal layers where they can respond to nerval and hormonal signals.
- *Iridophores* are smaller, round cells found in the dermal layers of fish. These cells contain platelets which reflect light resulting in a white/ silvery colour.
- *Xanthophores* and *erythophores* result in bright yellows, oranges and reds.

2.2. Origin of pigment cells and migration to the skin.

The identification of the neural crest, a transitory subpopulation of cells which develops above the neural tube in vertebrates, as the sole source of pigment cells was first established in amphibians [56] and then in other species. In fish, it is less clear as many species do not develop a distinct neural crest. It has, however, been clearly demonstrated in species such as the lamprey [46].

Pigment cell precursors migrate from the neural crest in a wave-like manner to uniformly seed the skin. It is thought that the various chromatophore types originate from a common neural crest precursor [3] and commitment to a specific type is not established until localization in the skin. The mechanisms controlling timing and migration of pigment cells from the neural crest are largely unknown. Cells do not acquire their characteristic pigment until after migration has ended, yet a number of markers have been developed which allow identification prior to pigment accumulation. A number of candidates have been proposed to control timing and migration of pigment cell precursors, including (i) a change in composition of the extra cellular matrix, (ii) the appearance of chemoattractant/repellent molecules, (iii) a change of cell adhesion properties. It is also possible that neural crest cell precursors may be forced onto a specific pathway due to the unattractive nature of other regions.

Studies of mouse mutations affecting coat pigmentation have provided an important tool for understanding factors involved in melanocyte development. Two essential receptor-ligand interactions have been revealed: the receptor tyrosine kinase, c-kit, with its ligand Steel factor (SLF, also called stem cell factor), e.g. [21, 64] and the endothelin receptor B together with endothelin 3 [5]. Soluble steel factor appears to have a role in regulating melanocyte precursor dispersal from the neural crest, whereas membrane-bound Steel factor is required for survival of the precursors within the dermis [63]. In addition to these observations, exogeneous SLF has been shown to be important for proliferation and differentiation of the melanocytes [31]. Intriguingly, SLF may have a role in promoting chemotactic activity in melanocytes, [20, 63, 31]. Cells expressing functional c-kit receptors may be selectively attracted onto the lateral pathway by SLF, which diffuses from its site of production in the dermatomal epithelium.

In addition to SLF, a number of melanocyte mitogens (chemicals inducing cell division) have been identified, including leukotrines, endothelin-1 and certain fibroblast growth factors [39, 54, 23, 65]. Several of these have additionally been shown to induce melanocyte chemotaxis and chemokinetic movement [24].

2.3. Formation of colours, patterns and colour change.

When one area of the skin is dominated by a specific colour, this can be attributed to an accumulation of pigment cells of the type producing that colour. White stripes (such as those on growing *Pomacanthus*) are often due to an abundance of iridophores, the red spots of certain carp are local aggregations of erythophore cells and black stripes in the angelfish are due to melanphores.

Despite few available pigments, a brief glance through an encyclopedia of

fishes [9] reveals a staggering number of different colours. The macroscopically perceived colour can be attributed to the microscopic organization of pigment cells in the skin. In amphibians and reptiles, chromatophores are arranged in ordered layers in the dermis to form the *dermal chromatophore unit*, [2]. These structures can create colours like green which cannot be formed by the available pigments alone. Similar arrangements exist in fishes. For example, blues of the damselfish are derived by a layer of iridophores backed by a layer of melanophores, [26, 19].

Increases and decreases in the number of dermal chromatophores leads to morphological colour changes. The changes result from proliferation of chromatophores and/or the degradation of terminally differentiated pigment cells [53]. By counting the number of chromatophores over a long period of adaptation to light or dark backgrounds in *Oryzias*, it has been shown that dark adaptation occurs via increased numbers of melanophores and decreased numbers of leucophores, and *vice versa* for the reverse process [58].

The interactions and mechanisms which lead to pattern formation remain largely unknown, however establishment of patterns in larval salamanders has received attention. In the larval salamander *Ambyostoma tigrinum tigrinum*, melanophores scatter uniformly over the flank of the embryo, while xanthophores remain in aggregates in premigratory positions. As the xanthophores migrate, the melanophores recede short distances to form alternating bars [11, 47, 51]. At this time, a horizontal stripe over the lateral surface of the myotomes develops which is free of the otherwise abundant melanophores. A series of experiments [52] suggest that several factors are involved in development of this stripe, including interactions between xanthophores and melanophores and extracellular factors. The melanophore free region appears to develop through active retreat of melanophores from the forming lateral line. The horizontal stripes in other salamanders are thought to develop by response of pigment cells to cues in the ECM, [60, 11].

2.4. Reaction-diffusion models in pigmentation.

Turing [61] demonstrated that a simple system comprising of two reacting and diffusing chemicals can, under appropriate conditions, lead to stationary nonhomogeneous patterns. This was proposed by Turing as a mechanism for morphogenesis. The application of Turing patterns to pigmentation was made by Murray [40, 41, 42, 43]. In essence, Murray proposed that a reaction-diffusion mechanism provides a morphogen prepattern which dictates cell differentiation. An attractive part of this theory is that the majority of mammalian patterns can be generated by such a mechanism. Similar models have been proposed by Bard [4] and Young [66].

The first modelling attempt to fish pigmentation patterns via reaction-diffusion theory was proposed by Kondo and Asai [29]. After observing the relationship between fish size and the number of stripes in the marine angelfish, *Pomacanthus semicirculatus*, a Turing model was proposed which predicts the doubling of the

number of peaks of chemical concentration as the domain length doubles. A comparison of stripe rearrangement in adult *P. imperator* and numerical simulations of the model showed close agreement. Attempts to address additional aspects of pigmentation in *Pomacanthus* have since been proposed. Varea *et al.* [62] considered domains whereby one side is shaped to reflect the curved geometry of the fish skin. Through considering "enhanced" boundary conditions such that model parameters are elevated along certain boundaries, they have demonstrated several additional aspects of *Pomacanthus* patterning, such as the complicated patterns seen along boundary edges in *Pomacanthus imperator* and the orientation of stripes with respect to the boundary. Painter *et al.* (1999) have augmented the model to include cell movement. This model is able to replicate the slow insertion of new stripes between older stripes. Additionally, features such as the curvature of juvenile stripes and the transition from stripes to spots as *P. semicirculatus* matures to adult have been shown in this model.

An activator inhibitor model has also been applied to the shell patterns of mollusks. The book by Meinhardt [38] demonstrates how many of the shell patterns seen in nature can by replicated in a reaction-diffusion model.

3. The cell movement model.

In this section we consider a mathematical model for pigment pattern formation in the skin of fishes. In this model, the following aspects are taken into account:

- When a specific area of the skin is dominated by one colour, it is due to an aggregation of chromatophores of the type producing that colour.
- Morphological colour changes of the skin are due to an increased population of chromatophores. We should mention, however, that such colour changes can also be brought about by increased deposition of pigment in epithelial cells.
- Patterning in the skin is controlled by distribution of one or more chemical factors. A number of candidates have been discovered, yet no definitive identity exists for a so-called morphogen. Kirschbaum [28] demonstrated via transplantation experiments that differentiation of melanophores in the zebrafish occurred through response to local cues in the dermis.
- Increases in the total number of pigment cells are via a combination of proliferation from chromatophores or from undifferentiated stem cells. The stem cells are undifferentiated pigment cell precursors. Further differentiation of stem cells into a specific pigment cell type is likely to result from extracellular factors in the dermis/extracellular matrix.
- Initial pigment cell distribution varies from species to species. In the zebrafish, the larval pigment pattern consists of four lateral lines of melanophores: dorsal, septal, abdominal and ventral. Pigment cells in larval *Pomacanthus arcuatus* initially form a uniform gray pigmentation when the fish is between 5 and 7 mm in length. The juvenile pigment pattern con-

sisting of five vertical white bars develops from this uniform distribution [27].

- Several lines of evidence point to chemotactic guidance of migrating melanocyte precursors from the neural crest to the dermis [10, 6, 59, 20]. Potential chemoattractants include steel factor [31] and endothelin-1 amongst others, [24]. In reality, cell movement may be induced by many mechanisms, including random motility, haptotaxis and cell adhesion.

Very little is currently known concerning the various interactions between the cell types, between the cells and the chemicals, and between the chemicals with each other, and it is not feasible at this moment to develop a highly detailed model for pigmentation patterning. We shall restrict attention to simple models of patterning which replicate the biological data.

In this section we consider a mechanism for generating the striped patterns in *Pomacanthus* based on a model for cell movement in response to gradients of chemical prepatterns derived from the reaction-diffusion system. The dominant chromatophore types involved in juvenile stripe development are likely to be melanophores, which we denote $M(\mathbf{x}, t)$, and iridophores, $I(\mathbf{x}, t)$. During the transition to adult stages, it is probable that other chromatophore types become important, and the effects of these may be a factor in the observed transformation. For example, yellow horizontal stripes of *P. imperator* are likely to be derived from xanthophores. In this model, we make the simplification of assuming that just one cell type is chemotactic, and that it is chemotactic to a single chemical species. Here we assume it is the iridophore cells, although we could equally postulate that it is the melanophores without qualitative differences in model behaviour. On a fixed domain, Ω, the equations are given by

$$\begin{aligned}
\frac{\partial M}{\partial t} &= -\nabla \cdot J_M + f_M(M, u, v), \qquad (3.1)\\
\frac{\partial I}{\partial t} &= -\nabla \cdot J_I + f_I(I, u, v),\\
\frac{\partial u}{\partial t} &= D_u \nabla^2 u + f(n, u, v),\\
\frac{\partial v}{\partial t} &= D_v \nabla^2 v + g(n, u, v).
\end{aligned}$$

J_M and J_I are flux terms for the melanophores and iridophores, respectively, and this contains contributions from random cell movement from chemotaxis. We simplify the model by assuming that only the two cell types reside in the dermis, and that the total cell density remains constant. Therefore, on a constant sized domain, we can take $f_M = f_I = 0$ (proliferation and degradation of pigment cells balance) and $\nabla \cdot (J_M + J_I) = 0$. Thus, melanophores themselves do not respond to the chemical gradients, however they experience a chemotactic flux type component through displacement by the moving iridophore cells. Zero flux is assumed at the boundary.

3.1. Patterning for different growth types.

During embryonic and juvenile stages, animals undergo considerable tissue growth and deformation. The effects of such growth on patterning is beautifully illustrated by the evolving pigmentation patterns seen on species of amphibia, reptiles and fish and, clearly, models proposed to explain features of embryonic development must consider the potential effect of domain growth on the patterning process. For example, by considering the growth of the developing alligator jaw, it has been demonstrated that a simple reaction-diffusion type mechanism may account for the sequence of tooth primordia, [30]. The need to consider the effects of growth on patterning has been illustrated for the reaction-diffusion mechanism on one and two-dimensional domains, [50, 49]. In one dimension, patterning such that the number of concentration peaks developing through the reaction-diffusion mechanism evolves through the mode doubling sequence $1-2-4-8-\ldots$ only occurs for certain parameters. In two dimensions, faster rates of growth can lead to highly convoluted stripes or no spatial pattern at all, rather than a regular pattern of stripes.

In the models considered to date domain growth has been incorporated in a simple manner, and a rigorous incorporation of tissue growth and deformation has yet to be undertaken. Even under a simple treatment it is possible to demonstrate that different types of domain growth may lead to very different patterning. This is demonstrated in the following example for a reaction-diffusion equation. Suppose evolution of a chemical, denoted by $c(\mathbf{x},t)$, evolves on the constant domain according to

$$\frac{\partial c}{\partial t} = D\nabla^2 c + f(c).$$

If we assume that Ω changes as a function of time, then it is straightforward to show through application of Reynolds Transport equation [**?**, 8]

$$\frac{\partial c}{\partial t} + \nabla\cdot\mathbf{u}c = D\nabla^2 c + f(c), \tag{3.2}$$

where $\mathbf{u} = \partial\mathbf{x}/\partial t$ defines the fluid flow. We consider two simple types of growth for a growing one-dimensional domain, $[0, L(t)]$.

3.1.1. Uniform growth.

For uniform growth, we assume for $x_i(0) \in (0, L)$, $x_i(t) = x_i(0)L(t)/L(0)$. Clearly, we have $u = xL'/L$, (where L' is the derivative with respect to t), and Equation (3.2) is given by,

$$\frac{\partial c}{\partial t} + \frac{cL'}{L} + \frac{xL'}{L}\frac{\partial c}{\partial x} = D\frac{\partial^2 c}{\partial x^2} + f(c).$$

We can convert the above equation on a one-dimensional growing domain onto a domain of constant size by the transformation, $(x,t) \to (y,\tau) = (x/L(t), t)$. It is easy to demonstrate that this transformation leads to

$$\frac{\partial c}{\partial t} = \frac{D}{L^2}\frac{\partial^2 c}{\partial y^2} + f(c) - \frac{L'}{L}c.$$

The uniform domain growth model leads to an equation for evolution of pattern in the reaction-diffusion system which can be solved with a simple numerical scheme. This may represent a good approximation for growth of the skin, were we to assume that nutrients required for cell proliferation were supplied uniformly to the skin from beneath. It is, however, a simplification of domain growth in living systems. Experimental data collected on growth of zebrafish and related species through larval and juvenile stages to adult [35] indicate that different regions of the body are growing at different rates.

3.1.2. Boundary growth.

Under boundary growth, we assume that for $x_i(0) \in (0, L)$, $x_i(t) = x_i(0)$. This represents growth at the boundary and we have $u = 0$. We follow the above procedure and use the same transformation onto a domain of constant size. This gives the following equation defining pattern evolution,

$$\frac{\partial c}{\partial t} = \frac{D}{L^2}\frac{\partial^2 c}{\partial y^2} + \frac{yL'}{L}\frac{\partial c}{\partial y} + f(c)$$

Boundary growth occurs during extension of the developing axons in the nervous system. The developing neuron consists of a nerve cell body (or soma), a long thin axon and, at the axon tip, the growth cone from which filopodia extend to sense the environment for guidance signals. Growth of the axon occurs at the level of the growth cone, [22]. Boundary growth may also be important with respect to skin growth if the nutrients were supplied from specific body regions.

3.1.3. Simulations under uniform and boundary growth.

We compare the different types of growth above by numerical simulation. Kinetics for the reaction-diffusion system are based on a two-species system proposed by Lengyel and Epstein [32] to account for spatial patterns generated in the CIMA chemical reaction, [7, 48]. The model is,

$$\begin{aligned} \frac{\partial u}{\partial t} &= D_u\frac{\partial^2 u}{\partial x^2} + k_1 - u - \frac{4uv}{1+u^2} \\ \frac{\partial v}{\partial t} &= k_3 D_v\frac{\partial^2 v}{\partial x^2} + k_2 k_3\left(u - \frac{uv}{1+u^2}\right) \end{aligned} \tag{3.3}$$

where D_u, D_v, k_1, k_2, k_3 are all positive constants. It is straightforward to determine the parameter space for Turing patterning.
In Figure 1 we compare results of numerical simulations for the following four cases:

- Exponential uniform and boundary growth $L(t) = L_0\exp(rt)$, Figure 1 (a) and (b).
- Linear uniform and boundary growth $L(t) = L_0(1 + rt)$, Figure 1 (c) and (d).

Under uniform exponential domain growth, Figure 1 (a), we see the mode doubling sequence of patterning which has been described previously, [1, 29, 50],

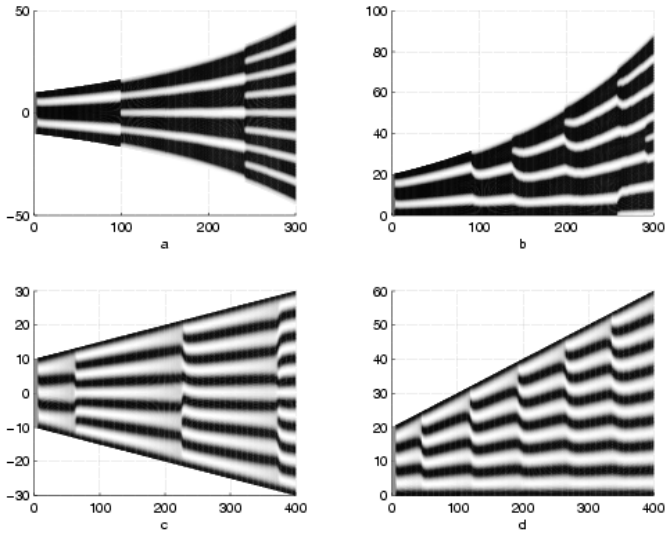

FIG. 1. *Chemical (u) concentrations on a domain growing in time, (horizontal axes represents time, vertical axes represent space), for the four cases in the text. (a) Exponential uniform growth, (b) Exponential boundary growth, (c) Linear uniform growth, (d) Linear boundary growth. Parameters $k_1 = 30.0$, $k_2 = 2.1$, $k_3 = 8.0$, $D_u = 1.0$, $r = 0.001$, $L_0 = 20.0$. Each time unit in the figure represents 5 units of simulation time. Numerical simulations are solved with an adapted Euler method, with zero flux boundary conditions and random perturbations about the homogeneous steady state for initial conditions.*

and proposed to provide a mechanistic basis for the doubling of the number of stripes as juvenile *Pomacanthus* doubles in length. With exactly the same parameters and conditions, yet using the boundary growth model, the regular sequence observed for uniform growth is lost. Initially new peaks/troughs develop near the growing boundary, however as the domain gets larger these are inserted in an irregular manner, Figure 1 (b).

We have used exponential boundary growth to make a direct comparison with the results of simulations under exponential uniform growth. However, such growth is biological unrealistic, as it implies that the rate at which new tissue is added at the boundary occurs at a faster rate as time increases. A more plausible boundary growth would be linear, representing a constant rate of increase at the boundary. In Figure 1, (c) and (d), we compare the uniform and boundary growth respectively for a linear function $L(t)$. With uniform linear growth, the regular sequence of mode doubling observed under exponential growth is lost. A regular sequence of patterning, however, now emerges for the linear growth under boundary growth. Peak splitting always occurs in the peak adjacent to the

growing boundary, and those further from the growth retain their spatial location throughout growth. Thus the patterning of peaks evolves in the sequence $3-4-5-6-7-8-\ldots$.

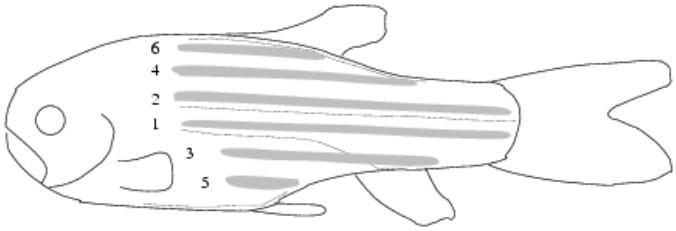

FIG. 2. *Order of adult stripe development in the zebrafish. Stripes 1 and 2 appear almost simultaneously from larval lines (dashed). Subsequent stripes appear in the order indicated.*

This latter behaviour is reminiscent of the mechanism by which new stripes emerge along the body of the adult zebrafish, Figure 2. Stripes 1 and 2 appear simultaneously from the larval pattern. Additional stripes appear in a specific sequence: 3 appears ventrally of 1, 4 appears dorsally of 1, 5 appears ventrally of 3, and 6 appears dorsally of 4. Stripes continue to be added, retaining this sequence, as space dictates. This sequence may suggest that growth in the zebrafish may be more closely approximated by boundary growth along the dorsal and ventral edges.

In summary, via the two types of growth we can force the patterning into different types of sequence. In boundary growth, the number of peaks of the reaction-diffusion sequence progress through the order $1-2-3-4-5-6-...$, whereas exponential uniform growth gives a peak doubling sequence $1-2-4-8-16-\ldots$.

3.2. Chemotactic-cell model under uniform growth.

We consider numerical simulation of the full chemotactic-cell model with a uniformly growing domain incorporated. A detailed investigation into the various behaviours this model can show has been presented elsewhere, [50]: Here we briefly explain how this model replicates the patterning phenomena of juvenile *Pomacanthus* development. The growth here is classified as *logistic*, stipulating that initially the fish grows in a manner approximating exponential growth, but eventually the growth rate slows and the fish approaches a maximum size.

This section considers two model formulations: (i) The zero cell feedback model, and (ii) the cell feedback model. In the former we have no effect on the chemicals by the cells: Chemical concentration patterns evolve independently and cells move in response to the gradients. In the second model we consider a form of chemical regulation by the cells by control of the rate of chemical synthesis. For the two-dimensional growing domain, $[0, L_1(t)] \times [0, L_2(t)]$, scaled onto a

domain of constant size, we have

$$\frac{\partial I}{\partial t} = \frac{1}{L_1^2}\frac{\partial}{\partial x}\left(D_I\frac{\partial I}{\partial x} - \frac{\chi_0}{(K+u)^2}I\frac{\partial u}{\partial x}\right) + \frac{1}{L_2^2}\frac{\partial}{\partial y}\left(D_I\frac{\partial I}{\partial y} - \frac{\chi_0}{(K+u)^2}I\frac{\partial u}{\partial y}\right)$$
$$\frac{\partial u}{\partial t} = D_u\left(\frac{1}{L_1^2}\frac{\partial^2 u}{\partial x^2} + \frac{1}{L_2^2}\frac{\partial^2 u}{\partial y^2}\right) + K(I) - u - \frac{4uv}{1+u^2} - (r_1+r_2)u,$$
$$\frac{\partial v}{\partial t} = k_3 D_v\left(\frac{1}{L_1^2}\frac{\partial^2 v}{\partial x^2} + \frac{1}{L_2^2}\frac{\partial^2 v}{\partial y^2}\right) + k_2 k_3\left(u - \frac{uv}{1+u^2}\right) - (r_1+r_2)v, \quad (3.4)$$

where $L_1(t) = L_2(t) = L_0\exp(rt)/(a+\exp(rt))$. See [50] for a derivation of these equations. We consider zero flux boundary conditions, and initial conditions weighted such that a stripe pattern will initially form.

3.2.1. Case 1: No cell feedback, $K(I) = constant = k_1$.

Simulations in this case have been described previously, [50], and a succession of frames at different times are plotted in Figure 3 for the chemoattractant, u, (a) – (e), and the cell density, (f) – (j). Chemical concentrations evolve through a stripe doubling sequence and, with no feedback from cells to chemicals, cells will simply move in response to the morphogen gradients. This creates stripes appearing faint and narrow at first, but growing with time. As the domain approaches the maximum size, the regular sequence of stripes breaks into a pattern of spots. Domain growth appears to hold the stripe pattern during initial stages, but as the the domain approaches its maximum size, the pattern relaxes to its favored Turing wavelength. This has been compared to the sequence of stripes forming in juvenile *Pomacanthus semicirculatus* and the subsequent transition to the spotted adult pattern. During the transition from juvenile to adult pattern, a "mixed pattern" is observed whereby the iridophores are reorganizing into spots, yet the stripes of the juvenile can still be seen. Such "transition patterns" are also observed during the transition from juvenile to adult pattern in *semicirculatus*. These transition stages are compared in Figure 4.

To understand the effects of differing chemotactic strengths, we vary the parameter χ_0 and examine the resulting cell density patterns. One dimensional results for three separate simulations are shown in Figure 5. For the "normal" chemotactic sensitivities, we observe the slow insertion of new stripes, consistent with the patterning on *Pomacanthus*. Similar patterning is observed when varying χ_0 by plus or minus an order of magnitude. Increases of χ_0 by plus or minus two orders of magnitude, however, result in very different patterning. In Figure 5 (b), χ_0 has been increased by two orders in magnitude. Although initial peaks develop as previously, no new stripes form. Due to the strong chemotactic effect, all available iridophores are pulled into the initial stripes, leaving few to create secondary stripes. A decrease by two orders of magnitude, (c), results in the disappearance of pattern. When the chemotactic effect is very weak, emerging cell aggregates have small amplitudes, such that they are likely to be indiscernible at the macroscopic level.

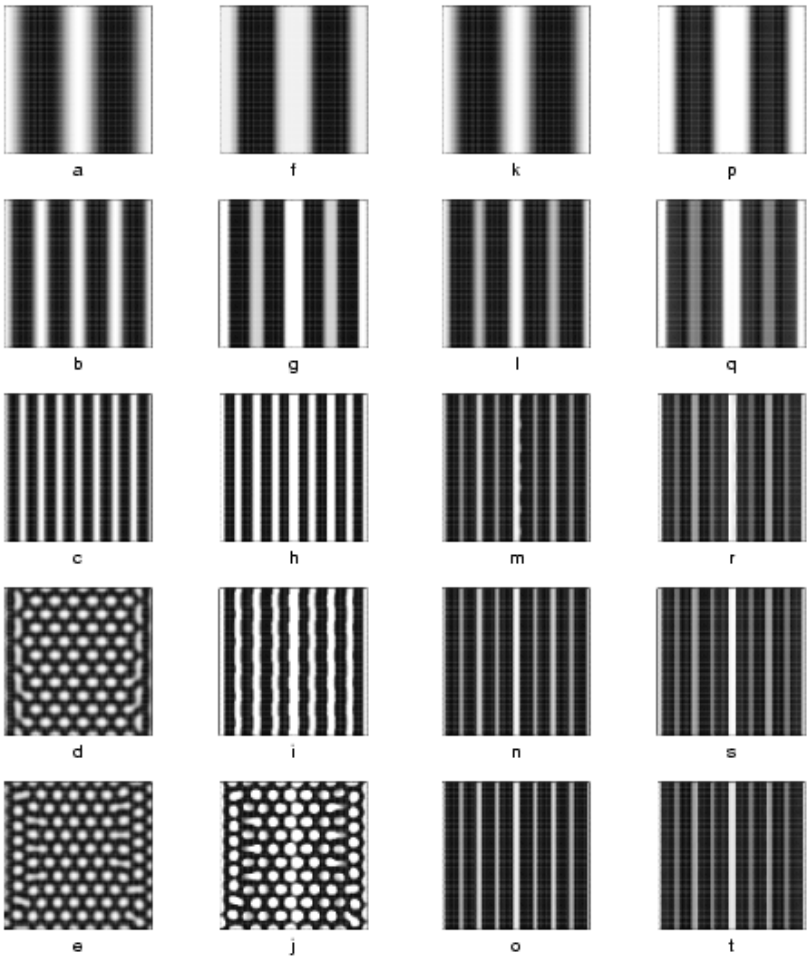

FIG. 3. *Numerical simulations for the cell movement model on a growing two-dimensional domain. For convenience of representation, the growing domain has been scaled onto one of constant size. (a) – (j) The zero feedback model shown for chemical* u*, (a) – (e), and cell density, (f) – (j), at* $t = 200$*, (a) and (f),* $t = 1600$*, (b) and (g),* $t = 3600$*, (c) and (h),* $t = 4200$*, (d) and (i), and* $t = 5200$*, (e) and (j). Corresponding plots for the feedback model are shown in (k) – (t). We use* $k_1 = 10.0$*,* $k_2 = 2.2$*,* $k_3 = 8.0$*,* $D_u = 0.01$*,* $D_v = 0.25$*,* $D_I = \chi_0 = 5.0 \times 10^{-5}$*.* $r = 0.001$*,* $a = 6.0$*,* $L_0 = 1.6$*,* $K = 1.0$*. Numerical simulations use an ADI method which has been adapted to include chemotactic cell movement.*

3.2.2. Case 2: Cell feedback, $K(I) = k_4 I/(1.0 + I)$**.** We consider the effect of a cell feedback which takes the form of regulation of chemical

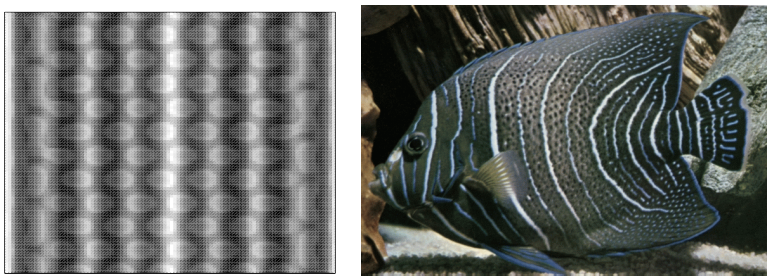

FIG. 4. *(a) Frame from the numerical simulation of Figure 3, (f) – (j), showing the transition of cell density during the change from a striped to spotted pattern. The slow movement of cells results in intermediate patterns consisting of both stripes and spots. Such patterns are observed between frames (i) and (j) of Figure 3. (b)* Pomacanthus semicirculatus *also shows such transition patterns during the establishment of the adult coloring. Other details as for Figure 3.*

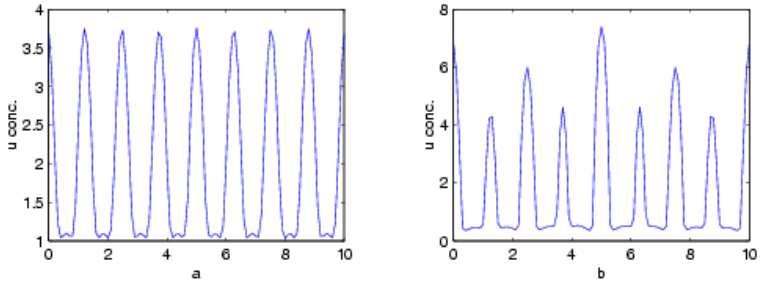

FIG. 5. *One dimensional space (vertical) - time (horizontal) plots for the cell density under varying chemotaxis strengths. In (a) we show the "standard" patterns with χ_0 set to 0.005 and other parameters as below. In (b), we use $\chi_0 = 0.5$. Here, the chemotaxis is strong and all available cells are pulled into the initial stripes. In (c), $\chi_0 = 0.00005$. Here, chemotaxis is weak such that the iridophore cell aggregations are indiscernible. Morphogen kinetics as used in Figure 3, $k_1 = 10.0$, $k_2 = 6.0$, $k_3 = 1.5$, $D_u = 0.01$, $k_3 D_v = 1.0$, $D_n = 0.001$ and $K = 10.0$. We use an exponentially growing domain, with growth rate $r = 0.01$ and an initial domain size of 1.6. White = cell density > 1.1, black = cell density <1.0.*

synthesis. Simulations are plotted in Figure 3, (k) – (o), for the chemical concentrations and in (p) – (t) for the cell density. The parameters, growth rates and the time at which the panels are plotted are the same as those in (a) – (j). Here we set $k_4 = 2k_1$, which reflects the same rate of chemical production at the cell density homogeneous steady state.

The addition of feedback results in notable differences to the zero feedback case. First, we observe increased stability of the striped pattern. With feedback, no breakdown of stripes into spots results as the domain approaches maximum size: The stripes remain in an 8 stripe pattern, seen in the zero feedback case prior to break-up. Intuitively, this may be explained since the cells provide an additional reinforcement of the stripes: to rearrange the pattern into one of spots means also moving the cells. The question of whether striped or spotted patterns arise in reaction-diffusion systems has been explored by several authors, [13, 33, 34, 44, 36], however at present it is not completely clear which pattern will develop for a general reaction-diffusion model.

A second difference between the two cases lies in the form of chemical patterns. With no feedback, the chemicals evolve as of a standard reaction-diffusion system. Consequently, on doubling of the number of chemical stripes, the new stripes that emerge have the same amplitude and width as pre-existing stripes, Figure 6 (a), see also Figure 1 (a). This inability to produce peaks of distinct "ages" was one of the criticisms of the model proposed by Kondo and Asai for angelfish stripes, [37, 50]. With chemical synthesis by cells, the underlying concentration peaks have clearly distinct amplitudes and widths, Figure 6 (b).

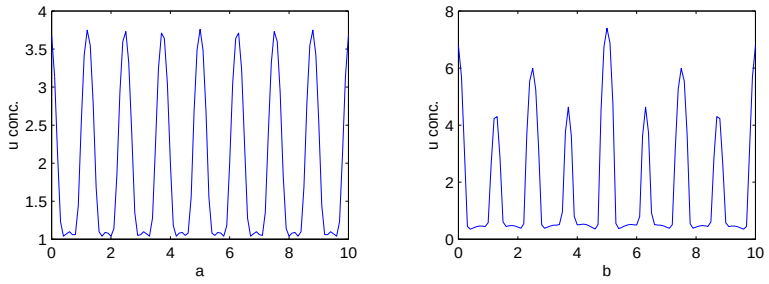

FIG. 6. *Comparison of the chemical concentration profiles at* $t = 4000$ *for the zero feedback model (a) and the feedback model (b), taken from the numerical simulations of Figure 3. The domain has grown from initial dimensions of* 1.6×1.6 *to* 10.0×10.0*. See text for details.*

3.3. Geometry of the domain.

To date, numerical simulations have been considered on either one-dimensional or two-dimensional domains of simple geometry (rectangular). As this is clearly a simplification of a real fish, we aim to understand the effects of realistic geometry on the patterning that develops.

3.3.1. Domain shape.

We explore the effects of domain shape on patterning. The tail fin patterns of *Pomacanthus* provide a relatively simple geometry which can be solved numerically. In Figure 7, (a) and (c), the results of two simulations under two sets of

initial conditions are considered. Those for (a) create highly curved stripes which results in complexity of pattern at the edges of the tail fin. This is compared with the patterning on the tail fin of *P. imperator*, (b). The initial conditions in (c) give rise to "gently" curved stripes, resulting in a simple pattern of curved stripes, as seen on the tail fins of juvenile *P. semicirculatus*, (d). For both simulations, the geometry of the domain affects the pattern that develops by arranging stripes perpendicular to the boundaries. This forces the stripes into maintaining curved patterns.

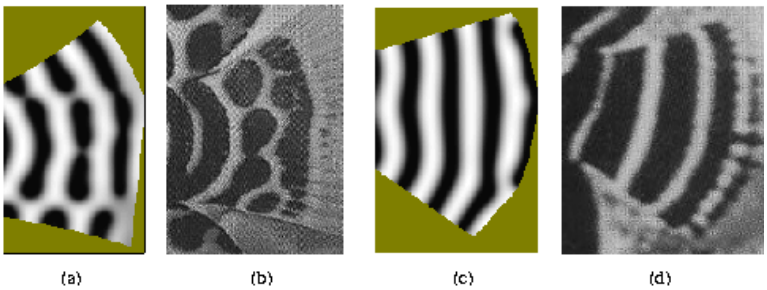

FIG. 7. *Comparisons of patterns of the reaction-diffusion model with* Pomacanthus *tail fins on a domain geometry reflecting the actual fin. Simulation, (a), and* P. imperator *tail fin, (b). Simulation, (c), and* P. semicirculatus *tail fin (d). The simulations in (a) and (c) have been obtained using slightly different sets of initial conditions, with the same reaction-diffusion model as considered before. Initial conditions in (a) give rise to more highly curved stripes. See (Painter* et al., *1999) for details. Parameters:* $k_1 = 30.0$, $k_2 = 1.95$, $k_3 = 8.0$, $D_u = 1.0$, $D_v = 1.5$.

The method of incorporating boundary shape has involved measuring dimensions of the fin from photographic images, calculating suitable functions to approximate the shape, and programming boundary conditions accordingly. This, of course, turns out to be a time-consuming and laborious process. A numerical scheme has been developed (see contribution by D. Bottino, this volume) which will solve a system of reaction-diffusion equations for a Voronoi tessellation. In Figure 8 (a), the result of a numerical simulation is shown, which solves the reaction-diffusion system given by Equations (3.3) on an irregular domain using this method. The boundary itself was created by tracing an image of a juvenile *P. semicirculatus* at 6 months old (shown in Figure 8 (b)) which is converted into a Voronoi grid by the scheme of Shewchuk, [57].

FIG. 8. *(a) Pattern generated by solving the reaction-diffusion system on the irregular domain determined by tracing the boundary of the real fish shown in (b). Equations solved using the numerical scheme of Bottino (see this volume) on a Voronoi grid. Figure (b) taken from Kondo and Asai (1995). Parameters:* $k_1 = 30.0$, $k_2 = 1.9$, $k_3 = 8.0$, $D_u = 0.0025$, $D_v = 0.0125$. *Initial conditions consider a disturbance of the homogeneous steady state in the area of the tail fin. This forces a pattern of curved stripes.*

3.3.2. Three dimensional patterning.

Fish chromatophore cells reside primarily in the dermis and, since body length and depth are much greater than the thickness of the skin, (on the order of 0.1-1 mm, although there is wide variation between species), it is often adequate to model two dimensions only. In some species, however, patterning occurs on a fine scale: the first two stripes appearing in zebrafish are approximately 1 mm apart. In such cases it may be necessary to consider three dimensions.

Numerical simulations for Turing structures developing in a two species reaction-diffusion mechanism on a three-dimensional domain are plotted in Figure 9. The two standard patterns are shown on thin layers: stripes and spots. Here, depth is small and has no effect on the patterning.

Depth has negligible effect on pigmentation when the reaction occurs uniformly throughout, but may play a role when non-uniformity of reaction is introduced. For example, if reactants come from lower layers, a gradient in the supply may occur. The potential effect can be understood by imposing a gradient on a parameter through the depth. Jensen *et al.* [25] considered such effects in two dimensions for the kinetics given by Equations (3.3) under variation of the parameter k_2. It was noted that structure of the pattern moved through regions of spatial homogeneity to spotted patterns to stripes. Variation of this same parameter in three dimensions shows similar transitions, as we show in various slices of the three dimensional pattern plotted in Figure 10. At lower k_2 the pattern consists of stripes, however as this is increased we observe transition to spots and homogeneity.

In summary, when a parameter varies through depth it may disrupt the patterning. This may be significant if the parameter region for patterning is small,

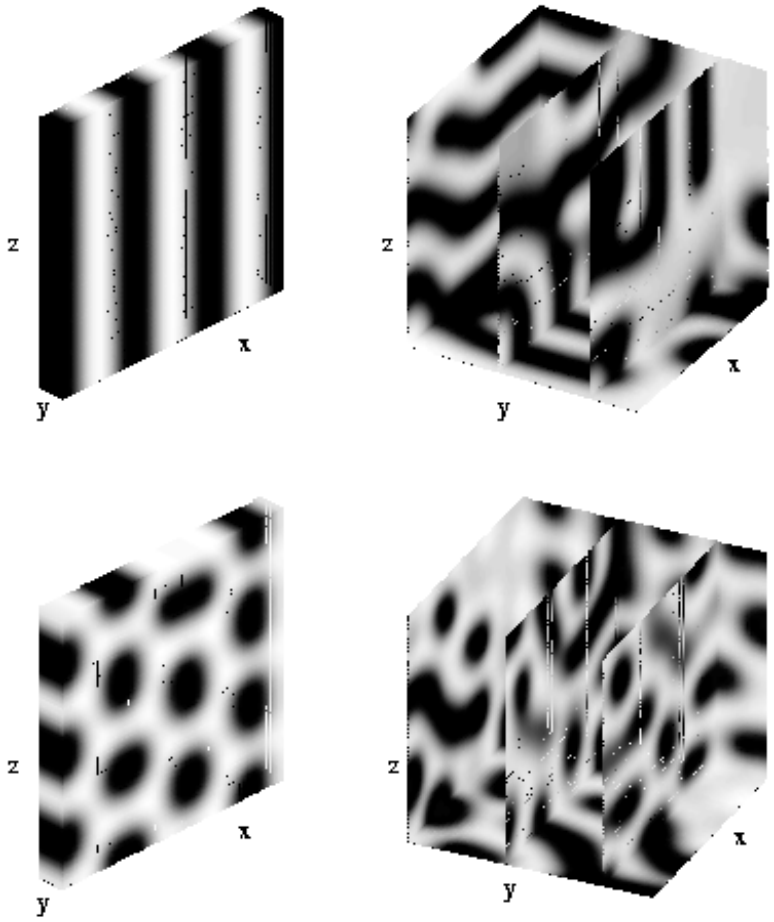

FIG. 9. *Three-dimensional patterns in a Turing system. Top left: On a thin domain, the pattern of stripes is maintained throughout the thickness of the domain. Bottom left: A similar effect occurs when the pattern is one of spots. Top and bottom right: Corresponding patterns for thicker layers. Slices through the pattern shows a large amount of structure and, in three dimensions, patterns show much less regularity than those in two dimensions. The regularity of the hexagonal patterns seen on the two dimensional layer is unlikely to develop when thickness becomes significant. Parameters use* $k_1 = 30.0$, $k_3 = 8.0$, $D_u = 1.0$, $D_v = 1.5$ *and* $k_2 = 1.4$ *for striped patterns,* $k_2 = 2.8$ *for spots. Equations solved using an Euler method with zero flux boundary conditions.*

in which case small variations in the parameter may shift the reaction outside the parameter space for patterning.

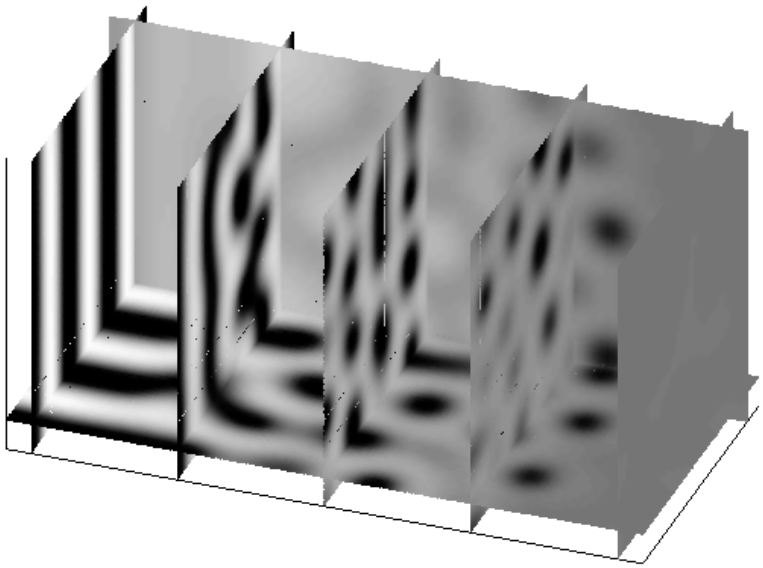

FIG. 10. *Simulations of three dimensional Turing patterns under linear variation of a kinetic parameter. Slices show how pattern varies along the direction of this variation. Patterning changes from stripes (left side) to spots (middle) and homogeneity (right). Simulations use the same kinetics as in previous simulations with* $k_1 = 30.0$, $k_3 = 8.0$, $D_u = 1.0$, $D_v = 1.5$ *and* k_2 *varies from 1.4 (left) to 5.6 (right). Domain dimensions are* $20 \times 40 \times 20$. *Solutions show pattern at* $t = 125$. *Simulations use an Euler method with zero flux boundary conditions.*

4. Discussion. In this article, recent experimental data on the development of skin pigmentation patterns has been reviewed. The mathematical model presented here and in earlier work, [50], has been shown to be capable of replicating many of the features observed during evolution of the pigment patterns in species such as *Pomacanthus semicirculatus*.

The understanding of patterns developing via a reaction-diffusion type mechanism on an irregular grid has received comparatively little attention to date. The development of numerical schemes in which a deforming irregular domain is considered will allow for simple incorporation of existing biological data on fish growth into the model and the understanding of pattern formation in such systems.

The modelling to date has considered a continuum approach to understand macroscopic patterning features. Experimental data in zebrafish and salamanders suggests that local interactions between pigment cell types may contribute to the patterning processes. One future direction is to employ a hybrid dis-

crete/continuum approach whereby cells are considered as discrete particles. This approach would allow understanding of how different types of microscopic rules for movement give rise to different macroscopic patterning.

A number of areas are open to theoretical treatment. As mentioned above, the question of whether stripes or spots occur in a general reaction-diffusion model has yet to be answered satisfactorily. Patterns have also been observed to undergo break up from regular stripes into convoluted stripes under various forms and rates of growth, [49, 50]. Whether these patterns represents a form of spatial chaos is an intriguing question.

The model has been shown to reproduce many of the features associated with pigmentation in *Pomacanthus semicirculatus*. A principal prediction of this and previous models is that the appearances of the new "interstripes" occurs when the fish has approximately doubled its previous length. Growth of angelfish in an aquarium environment is limited by the size of the tank (e.g. see [9]) and the above prediction could therefore be tested by limiting the growth rate of the fish in this manner. However, due to the slow rate of growth (approximately one and a half years to reach adult), large size (15 inches) and the territorial nature of *Pomacanthus*, these fish are unsuitable as laboratory animals. A more widely studied species is the zebrafish, *Danio rerio*, which is small, easy to breed and has a transparent skin allowing for relatively straightforward observations of cell movement and pattern formation. We are currently applying the model to pattern formation in the zebrafish to develop a number of experimentally testable predictions. Excision and transplant experiments, whereby a fragment of skin tissue from a donor is removed and either replaced at a new orientation or transplanted onto a host fish (which has also had a fragment of skin removed), can be easily performed within the modelling framework. Comparison of the model results with existing transplant experiments (e.g. [28]) in zebrafish, together with the development of new predictions will be used to test the suitability of the model as a mechanism for pigmentation.

The mechanisms underlying pattern formation in areas such as pigmentation are still poorly understood. For this reason, modelling thus far has concentrated on developing simple models which capture basic features of the patterning. As more sophisticated techniques become available, and many of the current ambiguities are resolved, the model will be adapted accordingly.

Acknowledgments I would like to thank D. Bottino for providing the numerical code and assisting me with simulations to solve the reaction-diffusion equations on an irregular grid.

REFERENCES

[1] P. Arcuri and J.D. Murray. Pattern sensitivity to boundary and initial conditions in reaction-diffusion models. *J. Math. Biol.*, 24:141–165, 1986.

[2] J.T. Bagnara and M.E. Hadley. *Chromatophores and Color Change*. Prentice-Hall, Eaglewood Cliffs, New Jersey., 1973.

[3] J.T. Bagnara, J. Matsumoto, W. Ferris, S.K. Frost, W.A. Turner, T.T. Tchen, and J.D. Taylor. Common origin of pigment cells. *Science*, 182:1034–1035, 1979.

[4] J.B.L. Bard. A model for generating aspects of zebra and other mammalian coat patterns. *J. Theor. Biol.*, 93:363–385, 1981.

[5] A. Greenstein Baynash, K. Hosoda, A Giaid, J.A. Richardson, N. Emoto, R.E. Hammer, and M. Yanagisawa. Interaction of endothelin-3 with endothelin-b receptor is essential for development of epidermal melanocytes and enteric neurons. *Cell*, 79:1277–1285, 1994.

[6] P. Blume-Jensen, L. Claesson-Welsh, A. Siegbahn, K.M Zsebo, B. Westermark, and C.I. Heldin. Activation of the human c-kit product by the ligand induced dimerization mediates circular actin reorganization and chemotaxis. *EMBO J.*, 10:4121–4128, 1991.

[7] V. Castets, E. Dulos, J. Boissonade, and P. De Kepper. Experimental evidence of a sustained standing turing-type nonequilibrium chemical pattern. *Phys. Rev. Lett.*, 64:2953–2956, 1990.

[8] E. Crampin, E. Gaffney, and P.K. Maini. submitted.

[9] N. Dakin. *The Macmillan book of the marine aquarium*. Macmillan Publishing Company, New York, 1992.

[10] N. M. Le Douarin. *The Neural Crest*. CUP, Cambridge, 1982.

[11] H.-H. Epperlein and J. Löfberg. The development of the larval pigment patterns in *triturus alpestris* and *ambystoma mexicanum*. *Adv. Anat. Embrol. Cell. Biol.*, 118:1–101, 1990.

[12] C.A. Erickson. From the crest to the periphery: Control of pigment cell migration and lineage segregation. *Pigment Cell Res.*, 6:336–347, 1993.

[13] B. Ermentrout. Stripes or spots? nonlinear effects in bifurcation of reaction-diffusion equations on the square. *Proc. Roy. Soc. Lond. A.*, 434:413–417, 1991.

[14] A. Fraser-Brunner. A revision of the chaetodont fishes of the subfamily *pomacanthinae*. *Proc. Zool. Soc.*, 36:543–596, 1933.

[15] A. Fraser-Brunner. Pattern development in the chaetodont fish *pomacanthus annularis* (bloch), with a note on the status of *euxiphipops*. *Copeia.*, 1:88–89, 1951.

[16] H.W. Fricke. Juvenile-adult colour patterns and coexistence in the territorial coral reef fish *pomacanthus imperator*. *Marine Ecology*, 1:133–141, 1980.

[17] R. Fujii. Cytophysiology of fish chromatophores. *Int. Rev. Cytol.*, 143:191, 1993.

[18] R. Fujii. *The Physiology of Fishes*, chapter Coloration and Chromatophores, pages 535–562. Marine Science Series. CRC press, Boca Raton, Ann Arbor, London, Tokyo, 1993.

[19] R. Fujii, H. Kasuwaka, , K. Miyaji, and N. Oshima. Mechanism of skin coloration and its changes in the blue-green damselfish. *Zool. Sci.*, 6:477–486, 1989.

[20] S.J. Galli, K.M. Zsebo, and E.N. Geissler. The kit ligand, stem cell factor. *Advances Immunol.*, 55:1–96, 1993.

[21] E.N. Geissler, M.A. Ryan, and D.E. Housman. The dominant-white spotting (w) locus of the mouse encodes the *c-kit* proto-oncogene. *Cell*, 55:185–192, 1988.

[22] S. F. Gilbert. *Developmental Biology*. Sinauer Associates, fifth edition, 1997.

[23] R. Halaban, S. Ghosh, and S. Baird. bfgf is the putative natural growth factor for human melanovytes. *In Vitro*, 23:47–52, 1987.

[24] T. Horikawa, D.A. Norris, J.J. Yohn, T. Zekman, and J.B. Travers J.G. Morelli. Melanocyte mitogens induce both melanocyte chemokinesis and chemotaxis. *J. Invest. Derm.*, 104:256–259, 1995.

[25] O. Jensen, E. Mesekilded, P. Borckmans, and G. Dewel. Computer-simulation of turing structures in the chlorite-iodide-malonic acid system. *Phys. Scripta.*, 53:243–251, 1996.

[26] H. Kasuwaka, N. Oshima, and R. Fujii. Mechanism of light reflection in blue damselfish motile iridophores. *Zool. Sci.*, 4:243–257, 1987.

[27] S. Kelley. Pigmentation, squamation and the osteological development of larval and juvenile gray angelfish *pomacanthus arcuatus* (pomacanthidae: Pisces). *Bull. Mar. Sci.*, 56(3):826–848, 1995.

[28] F. Kirschbaum. Untersuchungen uber dans farbmuster der zebrabarbe *brachydanio rerio* (cyprindae, teleostei). *Roux's. Arch. Dev. Biol.*, 177:129–152, 1975.

[29] S. Kondo and R. Asai. A reaction-diffusion wave on the skin of the marine angelfish *pomacanthus*. *Nature*, 376:675–768, 1995.

[30] P.M. Kulesa, G.C. Cruywagen, S.R. Lubkin, P.K. Maini, J. Sneyd, M.W.J. Ferguson, and J.D. Murray. On a model mechanism for the spatial patterning of teeth primordia in the alligator. *J. Theor. Biol.*, 180:287–296, 1996.

[31] T. Kunisada, H. Yoshida, H. Yamazaki, A. Miyamoto, H. Hemmi, E. Nishimura, L. D. Shultz, S. Nishikawa, and S. Hayashi. Transgene expression of steel factor in the basal layer of the epidermis promotes survival, proliferation, differentiation and migration of melanocyte precursors. *Development*, 125:2915–2923, 1998.

[32] I. Lengyel and I. R. Epstein. Modelling of Turing structures in the chlorite-iodide-malonic acid-starch reaction system. *Science*, 251:650–652, 1991.

[33] M.J. Lyons and L.G. Harrison. A class of reaction-diffusion mechanisms which preferentially select striped patterns. *Chem. Phys. Lett.*, 183:158–164, 1991.

[34] M.J. Lyons and L.G. Harrison. Stripe selection: An intrinsic property of some pattern-forming models with nonlinear dynamics. *Dev. Dyn.*, 195:201–215, 1992.

[35] M. McClure. *Chapter3: Growth, Shape Change, and the development of pigment patterns in fishes of the genus* Danio *(Teleostei: cyprindae)*. PhD thesis, Cornell University, 1998.

[36] H. Meinhardt. Models for positional signalling with application to the dorsoventral patterning of insects and segregation into different cell types. *Development*, supplement:169–180, 1989.

[37] H. Meinhardt. Dynamics of stripe formation. *Nature*, 376:722–723, 1995.

[38] H. Meinhardt. *The algorithmic beauty of sea shells*. Springer, Berlin, New York, 2nd edition, 1998.

[39] J.G. Morelli, J.J. Yohn, B. Lyons, R.C. Murphy, and D.A. Norris. Leukotrines c_4 and d_4 as potent mitogens for cultured human neonatal melanocytes. *J. Invest. Dermatol.*, 93:719–722, 1989.

[40] J.D. Murray. A pattern formation mechanism and its application to mammalian coat markings. volume 39 of *Lecture Notes in Biomathematics*, pages 360–399. Springer, Berlin, Heidelberg, New York., 1979.

[41] J.D. Murray. A pre-pattern formation mechanism for animal coat markings. *J. Theor. Biol.*, 88:161–199, 1981.

[42] J.D. Murray. How the leopard got its spots. *Sci. Am.*, 258:80–87, 1988.

[43] J.D. Murray. *Mathematical Biology*. Springer-Verlag, Berlin, Heidelberg, New York, second edition edition, 1993.

[44] B. N. Nagorcka. From stripes to spots: Prepatterns which can be produced in the skin by a reaction-diffusion system. *IMA. J. Math. Appl. Med. & Biol.*, 9:249–267, 1992.

[45] T. Naitoh, A. Morioka, and Y. Omura. Adaptation of a common freshwater goby, yoshinobori, *rhinogobius brunneus* temminck et schlegel to various backgrounds including those containing different sizes of black and white checkerboard squares. *Zool. Sci.*, 2:59, 1985.

[46] D.R. Newth. On the neural crest of the lamprey embryo. *J. Embryol. Exp. Morphol.*, 4:358–375, 1956.

[47] L. Olsson and J. Löfberg. Pigment pattern formation in larval ambystomatid salamanders: *Ambystoma tigrinum tigrinum*. *J. Morphol.*, 211:73–85, 1992.

[48] Q. Ouyang and H.L. Swinney. Transition from a uniform state to hexagonal and striped turing patterns. *Nature*, 352:610–612, 1991.

[49] K.J. Painter. *Chemotaxis as a Mechanism for Morphogenesis*. PhD thesis, University of Oxford., 1997.

[50] K.J. Painter, H.G. Othmer, and P.K. Maini. Stripe formation in juvenile *po-*

macanthus explained by a generalized turing mechanism with chemotaxis. Submitted article, 1999.

[51] D. M. Parichy. Pigment patterns of larval salamanders (ambystomatidae, salamandridae): The role of the lateral line sensory system and the evolution of pattern-forming mechanisms. *Dev. Biol.*, 175:265–282, 1996.

[52] D. M. Parichy. When neural crest and placoses collide: Interactions between melanophores and the lateral lines that generate stripes in the salamander *ambystoma tigrinum tigrinum* (ambystomatidae). *Dev. Biol.*, 175:283–300, 1996.

[53] G.H. Parker. *Animal Colour Changes and Their Neurohumours*. CUP, Cambridge, 1948.

[54] J.S. Rubin, A.M.L. Chan, D.P. Bottaro, W.H. Burgess, W.G. Taylor, A.C Cech, D.W. Hirschfield, J. Wong, T. Miki, P.W. Finch, and S.T. Aaronson. A broad spectrum human lung fibroblast-derived mitogen is a variant of hepatocyte growth factor. *Proc. Natl Acad. Sci. USA*, 88:415–419, 1991.

[55] M. Schliwa. *Biology of the Integument 2: Vertebrates*, chapter Pigment Cells, pages 65–77. Springer-Verlag, Berlin Heidelberg New York Tokyo, 1986.

[56] G. P. Du Shane. The origin of pigment cells in amphibia. *Science*, 80:620–621, 1934.

[57] Jonathan Richard Shewchuk. Triangle: Engineering a 2D Quality Mesh Generator and Delaunay Triangulator. In Ming C. Lin and Dinesh Manocha, editors, *Applied Computational Geometry: Towards Geometric Engineering*, volume 1148 of *Lecture Notes in Computer Science*, pages 203–222. Springer-Verlag, May 1996. From the First ACM Workshop on Applied Computational Geometry.

[58] M. Sugimoto. Morphological colour changes in the medaka, *oryzias latipes*, after prolonged background adaptation — i. changes in the population and morphology of the melanophores. *Comp. Biochem. Physiol.*, 104A:513, 1993.

[59] K. W. Tosney. A long distance cue from emerging dermis stimulates neural crest migration. *Soc. Neurosci. Abs.*, 18:1284, 1992.

[60] R. P. Tucker and C. A. Erickson. Pigment patternformation in *taricha torosa*: The role of the extracellular matrix in controlling pigment cell migration and differentition. *Dev. Biol.*, 118:268–285, 1986.

[61] A.M. Turing. The chemical basis for morphogenesis. *Phil. Trans. Roy. Soc. Lond. B.*, 237:37–72, 1952.

[62] C. Varea, J. L. Aragon, and R. A. Barrio. Confined turing patterns in growing systems. *Phys. Rev. E.*, 56:1250–1253, 1997.

[63] B. Wehrle-Haller and J.A. Weston. Soluble and cell-bound forms of steel factor activity play distinct roles in melanovyte precurso dispersal and survival on the lateral neuarl crest migration pathway. *Development*,

121:731–742, 1995.

[64] D.E. Williams, J. Eisenman, A. Baird, C. Ruach, K. Van Ness, C.J. March, L.S. Park, U. Martin., D.Y. Mochizuki, H.S. Boswell, G.S. Burgess, D. Cosman, and S.D. Lyman. Identification of a ligand for the *c-kit* proto-oncogene. *Cell*, 63:167–174, 1990.

[65] Y. Yada, K. Higuchi, and G. Imokawa. Effects on endothelins on signal transduction and proliferation in human melanocytes. *J. Biol. Chem.*, 266:18352–18357, 1991.

[66] D.A. Young. A local activator-inhibitor model of vertebrate skin patterns. *Math. Biosci.*, 72:51–58, 1984.